ISSN 1330-3651 (Print), ISSN 1848-6339 (Online)
https://doi.org/10.17559/TV-20230221000368
Preliminary communication

Effects of Altitude on Fire Smoke Diffusion in Semi-Lateral Smoke Exhaust Highway Tunnels

Xiaohua JIN*, Zhihao LIN, Shunheng HUA, Xinru TONG, Xiaoyan LI, Lingbo ZHANG, Jiankun GONG

Abstract: This paper aims to study the effects of altitude and the size of smoke outlet on fire smoke diffusion and discharge in semi-lateral smoke exhaust highway tunnels. At first, simulations of semi-lateral smoke exhaust highway tunnels were carried out in FDS (Fire Dynamics Simulator), then the distribution laws of temperature, CO concentration, smoke mass flow, and visibility in the tunnel under the conditions of different altitudes and smoke outlet areas were analyzed to figure out the effects of altitude and size of smoke outlet on fire smoke diffusion and discharge in the said tunnels. The results suggest that, in case of the same fire source power, the velocity of smoke diffusion increases with the altitude; for curves of different altitudes, the tunnel roof temperature features are basically the same, that is, the higher the altitude, the higher the temperature at the tunnel roof. When the fire source power is 20 MW, the smoke mass flow at the smoke outlet decreases with the increase of altitude, but the CO concentration grows with it, indicating that the smoke exhaust efficiency is higher in high-altitude areas. When the altitude reaches 4200 m and the fire source power is 20 MW, with the increase of smoke outlet area, the smoke discharge effect of the tunnel shows an upward trend, taking both the smoke discharge effect and economy into consideration; the smoke outlet should take a size of 4 × 3 m.

Keywords: altitude; size of smoke outlet; smoke control; tunnel fire simulation

1 INTRODUCTION

Facilities on highways in high-altitude areas of western China have been greatly improved in recent years as the initiative of common prosperity is being implemented in the country. According to *Statistics on the Development of the Transportation Industry in China in 2021* issued by the Ministry of Communications, by the end of 2021, the total mileage of highways in western China accounted for 42.8% of the total mileage of highways in the country, and the number has increased by 0.5% compared with that by the end of year 2020. Moreover, the total mileage of expressways in western China accounted for 41.3% of the total mileage of the country, and this number has increased by 1.7% compared with that by the end of 2020. Overall speaking, the gap of road network scale and facilities between western areas and the eastern and central areas of China has been narrowed down further. Western China is a mountainous area, in view of this situation, a large number of highway tunnels have been built in western China for the purposes of improving transportation efficiency and shortening the traffic distance. However, due to the long, narrow, and closed spatial structure of tunnels, in the event of a fire, a large amount of toxic and harmful gases will be generated in the tunnels. Research shows that toxic gases and high-temperature smoke generated by the fire are the main causes of casualties, and they are responsible for about 85% of the total casualties [1, 2]. The low pressure and low oxygen environment in high altitude areas pose a great threat to the fire safety of tunnels [3-5], so the research on fire smoke prevention and control in tunnels at different altitudes is a very meaningful work.

After carefully reviewing relevant studies, it is found that most of the existing works are for fire prevention and control in plain areas, only a small number of studies talk about fire burning features at high-altitudes. For instance, Tan et al. [6] analyzed the effects of ambient pressure on the mechanical smoke exhaust efficiency in case of tunnel fire with the help of FDS, and their simulation results show that the thickness of smoke layer in the tunnel increases with the decrease of ambient pressure. Yan et al. [7] also used FDS to perform numerical simulation on the effects of ambient pressure on smoke movement in fire shaft of natural ventilation tunnels, and found that as the ambient pressure decreases, the temperature and moving speed of smoke in the tunnel would both increase; in case of low heat release rates, the length of the reverse flow of the smoke increases with the decrease of ambient pressure. Ji et al. [8] used a self-built full-scale numerical simulation model to reveal the effects of ambient pressure on the movement and temperature distribution of fire smoke in tunnels, and they discovered that with the decrease of ambient pressure, the temperature in the vertical direction of the tunnel would rise accordingly. Scholar Huang et al. [9] simulated the fire dynamics in mines at different altitudes in FDS and found that the peak temperature and CO concentration of smoke would decrease with the increase of altitude. Wieser et al. [10] experimented on a 6 × 2.8 × 2.1 m reduced-size model of road tunnel, and found that within the 400~3000 m altitude range, with the increase of altitude, ambient pressure and oxygen density gradually decreased, resulting in a slowdown in the development of fire. Li et al. [11] used a reduced-size experimental platform to study the combustion characteristics of three gaseous hydrocarbon fuels at two different altitudes in Hefei and Lhasa of China, and found that, compared with normal pressure state, the heat release rate and combustion efficiency of the fire source in low pressure state have been improved to varying degrees, while the radiation fraction and radiation heat flow both decrease. Wang et al. [12] simulated a full-size aircraft cargo cabin and discovered that the plume coefficient of the cabin ceiling is lower than the entrainment coefficient of the plume, and it decreases gradually with the decrease of ceiling pressure and distance. Zhou et al. [13] used a self-built experimental device to study the influence of low pressure on heat release rate and revealed that the decrease of ambient pressure would cause the combustion efficiency and convection coefficient of the fire source to increase slightly, which will further lead to an increase in the heat release rate of the fire source. Chen et al. [14] studied the influence of ambient pressure on thermal runaway and ignition behaviour of lithium battery by means of

experimental measurement and theoretical analysis, and found that the different ambient pressures would result in different rupture temperature and time of safety valve, and the effective combustion under low pressure is lower than that under normal pressure.

In addition, through literature review, it is also found that most of the existing works focus on the effects of low pressure environment on the combustion characteristics of fuels such as methane, the combustion characteristics of batteries, the smoke exhaust of tunnel shaft, the fire in mine tunnels, or the combustion of aircraft cargo cabin, etc. [15-18]. Studies concerning the smoke exhaust of semi-lateral tunnels are mostly in plain areas [19-21], while the report of smoke exhaust of semi-lateral tunnels is rarely seen. Therefore, to fill in this research blank, this paper aims to study the fire smoke diffusion features of tunnels in high altitude areas with the help of FDS, formulate fire smoke prevention and control measures, and provide technical support for the selection of design parameters of semi-lateral smoke exhaust system in high altitude areas.

2 NUMERICAL SIMULATION AND CALCULATION PARAMETERS

2.1 Modelling

Referring to the experiment of Xu et al. [22], a semi-lateral highway tunnel model was built in Pyrosim. The size of the tunnel model was 180 m long, 12 m wide, and 5 m high. The center point of the tunnel was taken as the origin of the coordinates. The vehicle in fire was located on the center line of the tunnel, and its length, width and height are respectively 6 m, 2 m, and 2 m. The smoke outlets were directly above the center line of the tunnel, and were symmetrically distributed about the center point. According to stipulation of the *Highway Tunnel Ventilation Design Details*, the distance between two rows of smoke outlets should not be less than 60 m, so in the experiment, 60 m was taken as the spacing, as shown in Fig. 1.

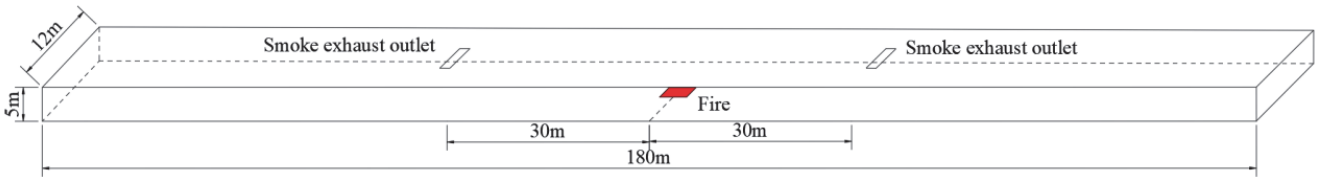

Figure 1 The tunnel model

2.2 Calculation Conditions and Measuring Point Arrangement

Vehicles passing through the tunnel highways are mostly cars, trucks and buses. According to NFPA502 [23] (Standard for Road Tunnels, Bridges, and Other Limited Access Highways) formulated by the National Fire Protection Association, the fire source powers of cars, trucks, and buses were set as 5 MW, 10 MW and 20 MW, respectively. Assuming: the fire source was located in the middle of two smoke outlets; the fuel of the fire source was n-heptane; steady-state fire was adopted; the power magnitude of the fire source does not vary with time; the burning of every kilo n-heptane would generate 6×10^{-3} kg CO and 0.015 kg soot [24]; the initial temperature of the tunnel was 20 ℃, all walls of the tunnel were set as "Concrete", the inlet and outlet at both ends were set as "Open", the smoke outlets were set as "Exhaust", and the amount of smoke discharged from the smoke outlets was set as 60 m^3/s per the stipulation of the *Highway Tunnel Ventilation Design Details*.

At plane $Z = 2$ m, measuring points of temperature, CO concentration, and visibility were set at intervals of 1m along the center line of the tunnel; at the 0.1m position under the tunnel roof, measuring points of temperature and CO concentration were set at 1m intervals along the center line of the tunnel; measuring points of CO, CO_2 and smoke mass flow were set on both left and right sides of the smoke outlets to observe the parameters of the smoke on the center line of the tunnel.

2.3 Meshing

FDS is a software used to simulate fluid motion in fire, study the heat transfer and smoke diffusion processes during fire, and experiment on fire in tunnels, subways, garages and other places, thereby providing theoretical support for scientific research on fire safety issues. According to the independent mesh size experiment of McGrattan et al. [25], it is found that the fluid viscous stress model can be accurately calculated only when the ratio of the fire source characteristic diameter D^* to the mesh size δ_x is between 4 and 16, Eq. (1) gives the formula for calculating the fire source characteristic diameter D^*:

$$D^* = \left(\frac{Q}{\rho_\infty c_p T_\infty g^{1/2}} \right)^{2/5} \tag{1}$$

where, D^* is the characteristic diameter of the fire source, unit is m; Q is the power of the fire source, unit is kW; c_p is the specific heat capacity at constant pressure, unit is kJ/(kg·K); ρ_∞ is environment density, unit is kg/m^3; T_∞ is environment temperature, unit is K; g is the acceleration of gravity, unit is m/s^3.

To set a proper size for grids, before simulation, the different grid sizes were simulated and verified. Four different grid sizes 0.167 m, 0.2 m, 0.333 m and 0.5 m were selected for simulation, at the same time, the smaller the combustion power of the fire source, the smaller the size of the grid, so take the minimum power of the fire source 5 MW as an example, the temperature changes of the tunnel roof right above the center point of the fire source under the condition of different grid sizes were observed, as shown in Fig. 2, the smaller the grid size, the smaller the fluctuation range of the temperature, and the more accurate the calculations. However, considering the running performance of the computer, a grid size of 0.333 m was adopted for the simulation, and the simulation time was 360 s.

2.4 Scheme Design and Simulation Conditions

In this study, the altitude of the tunnel and the area of smoke outlets were changed to simulate the smoke temperature, CO concentration, and visibility in the escape zone, and the simulation conditions are given in Tab. 1. The safe evacuation standards were set based on relevant specifications [26]: (1) The smoke temperature at 2 m height, namely the characteristic height of human eye, is lower than 60 ℃, the visibility is greater than 10m, and the CO volume fraction is not greater than 250×10^{-6} mol/mol; (2) The roof temperature is not higher than 180 ℃. Air pressure and air density at simulated altitude are shown in Tab. 2.

Table 1 Setting of simulation conditions

Condition No.	Fire source power / MW	Altitude / m	Size of smoke outlet / m × m
1-5	5	0/950/1850/2750/4200	4 × 1.5
6-10	10	0/950/1850/2750/4200	4 × 1.5
11-15	20	0/950/1850/2750/4200	4 × 1.5
16	20	4200	2 × 1.5
17	20	4200	4 × 1.5
18	20	4200	3 × 3
19	20	4200	4 × 3
20	20	4200	5 × 3
21	20	4200	6 × 3

Table 2 Simulation of air pressure and density at altitude

Altitude / m	Ambient Pressure / kPa	Ambient Oxygen Mass Fraction / kg/kg
0	101	0.232378
950	90	0.216
1850	80	0.1988
2750	70	0.18
4200	60	0.16

3 EFFECTS OF ALTITUDE ON SMOKE EXHAUST

3.1 Tunnel Smoke Temperature and Diffusion Comparison

When a fire breaks out in the tunnel, the generated smoke will form a plume and rise freely to the tunnel roof, then the plume of the smoke will move horizontally along the roof. The one-dimensional horizontal movement of the smoke is the longest stage of fire spread, and it is the best time period for smoke control and personnel evacuation. Fig. 3 shows the smoke diffusion in the tunnel at the 30th second of fire outbreak under the condition of different altitudes of 0 m, 950 m, 1850 m, 2750 m and 4200 m, as can be seen from the figure, at a same time moment, with the increase of altitude, the smoke diffusion distance gets longer, and the diffusion speed is faster. The reason is that as the smoke is spreading along the roof to the tunnel outlets, high temperature smoke gas and fresh air heat exchange, the temperature of the smoke gas gradually decreases, the thermal buoyancy also decreases; when the smoke gas reaches a certain height, the smoke gas will form a neutral surface between the air layer, the smoke gas will form a smoke gas layer, at the same time, the air coming from the outside of the tunnel moves from the outlets to the fire source to provide fresh oxygen for the combustion of the fire source. With the rise of the altitude of the tunnel, the content of oxygen in the air becomes smaller, and the ambient pressure decreases gradually in the meantime. To get more oxygen, the smoke will diffuse faster to increase the contact area with the air.

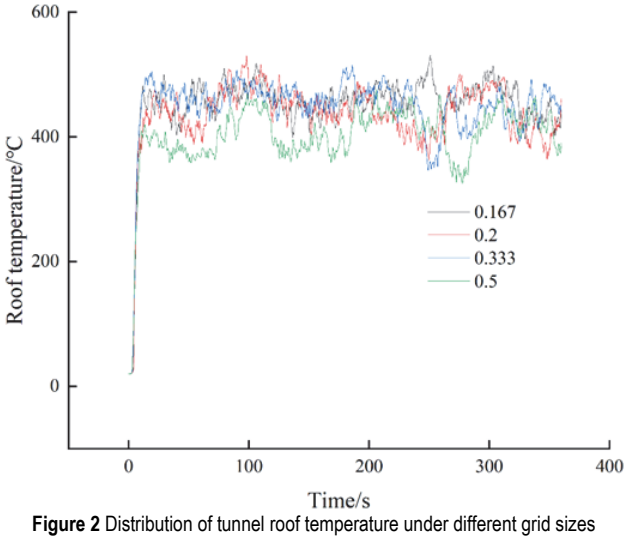

Figure 2 Distribution of tunnel roof temperature under different grid sizes

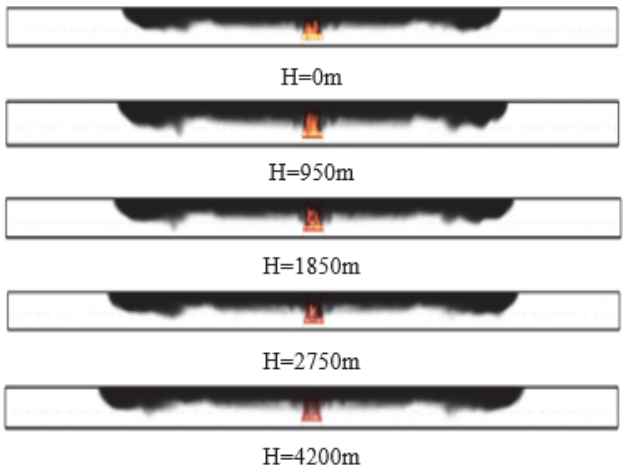

Figure 3 Smoke diffusion at different altitudes

The one-dimensional horizontal movement stage of fire smoke is the key stage of fire control, in the experiment, the power of the fire source was set to 20 MW, and the tunnel roof temperate at the 10th, 30th, 40th and 50th second of fire outbreak is shown in Fig. 4; after fire breaks out in the tunnel, a large amount of smoke generated by the fire will be accumulated at the roof, so the roof temperature can well reflect the smoke diffusion situations in the tunnel. As can be seen in the figure, the temperate curves of different time moments are basically the same; in high altitude areas, the reaction after fire outbreak is faster, and the smoke spreads faster as well, which poses greater challenges to fire prevention and control. At different time moments, the highest point of roof temperature appears directly above the fire source in the tunnel, and the higher the altitude, the lower the peak temperature. Although the peak temperature in high altitude areas is lower, the range of high-temperature zone is the same as that in low altitude areas, so it is suggested to use temperature difference sensors in high altitude highway tunnels and, if necessary, use smoke detectors that are more sensitive than those used in plain areas.

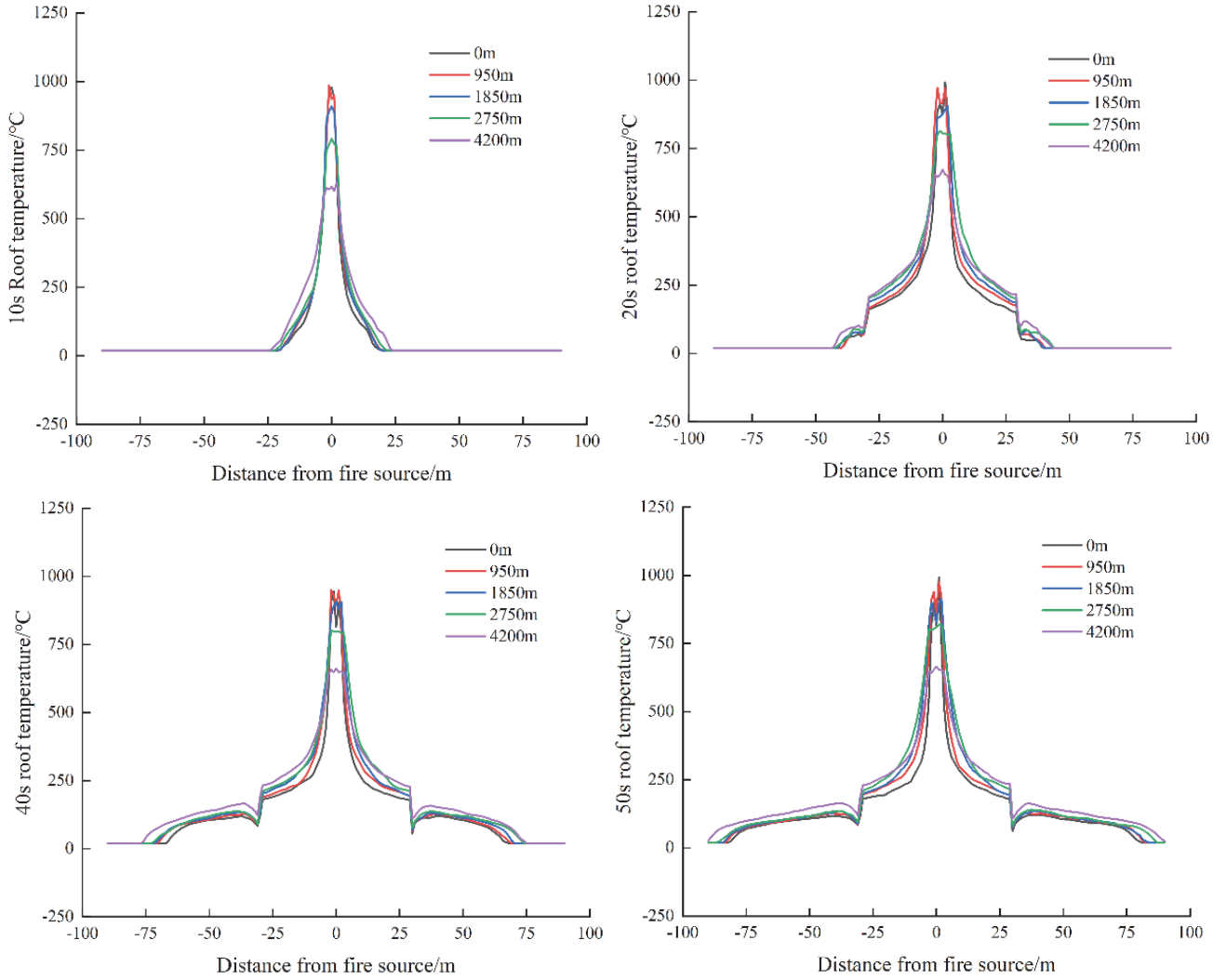

Figure 4 Roof temperature at different time moments

3.2 Roof Temperature in Escape Zone

The highest temperature in the road tunnel is located 0.05*H* below the roof (*H* is the height of the tunnel) The height of the tunnel set in this paper is 5 m, so the temperature on 0.01 m below the roof is the temperature of the roof. The development of fire in high altitude areas and in plain areas is the same, it can be divided into three stages: fire development stage, complete combustion stage, and attenuation stage. During the complete combustion stage, the combustion features of the fire tend to be stable, and the tunnel roof temperature reaches the maximum. Since the left and right of the tunnel are completely symmetrical, so the roof temperature of the right side of the tunnel has been taken for research. Fig. 5 shows the distribution of roof center line temperature under the condition of different altitudes and fire source powers, as can be seen from the figure, with the increase of distance, the roof temperature near the center point of the fire source shows a trend of increasing fast at first and then dropping gradually after reaching the peak; the main reason is that during the process of smoke spreading from fire source center to the tunnel outlet, the smoke exchanges heat with the surrounding walls and the cold air constantly, making the temperature to drop continuously. In the mean time, the temperature difference near the center point of the fire source is greater, this is because the heat convection and heat radiation between the smoke and the surrounding walls and cold air are more intense, which has resulted in a large temperature gradient near the fire source. The roof temperature curves of different altitudes have the same features, that is, the peak roof temperature decreases with the increase of altitude, while in areas far from the fire, the roof temperature increases with the altitude. This is because the air density and entrainment capacity of the smoke are two most important factors affecting roof temperature. With the increase of altitude, the oxygen content in the air exhibits a downward trend. When the altitude reaches 4200 m, the oxygen content in the air decreases by about 45% compared with the sea level, and the air density decreases gradually as well; at the same time, with the increase of altitude, the intensity of thermal stratification of the flue gas increases, which in turn leads to a gradual decrease in the roll absorption capacity of the flue gas and a smaller temperature drop of the smoke gas.

According to Fig. 5, at the altitude of 4200 m, the greater the fire source power, the higher the temperature of the roof smoke, and the peak roof temperature of a 20 MWfire source power is 176 ℃ higher than that of a fire source power of 5 MW. The reason is that the higher the fire source power, the more intense the combustion, the stronger the heat radiation and heat convection of the smoke, the higher the temperate of the smoke gas.

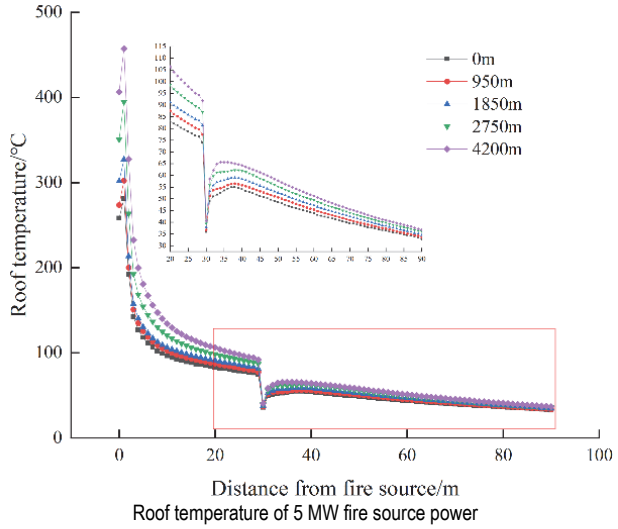

Roof temperature of 5 MW fire source power

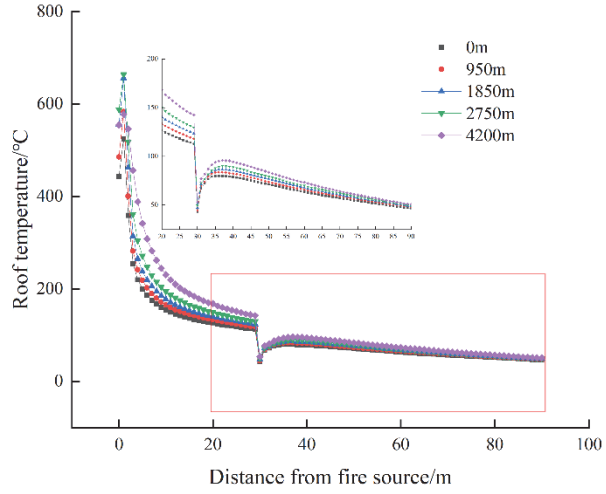

Roof temperature of 10 MW fire source power

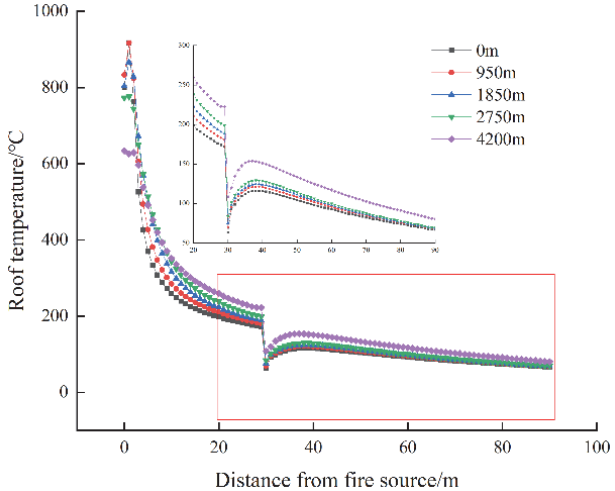

Roof temperature of 20 MW fire source power

Figure 5 Roof temperature at different altitudes

3.3 Smoke Mass Flow and CO Concentration at Smoke Outlet

Fig. 6 shows the smoke mass flow discharged from smoke outlet at different altitudes in case of a 20 MW fire source power. As can be seen in the figure, the smoke mass flow shows a decreasing trend with the increase of altitude; when the altitude is 4200 m, the smoke mass flow is 17.7 kg/s, which is 50.1% lower than that at low altitudes. Within the 0-2500 m altitude range, the trends of smoke mass flow are basically the same, while within the 2500-4200 m altitude range, the curve of smoke mass flow changes gently. This is because with the increase of altitude, both the density of oxygen in the air and the ambient pressure become smaller, which weakens the entrainment capacity of smoke gas, thereby reducing the amount of smoke discharge.

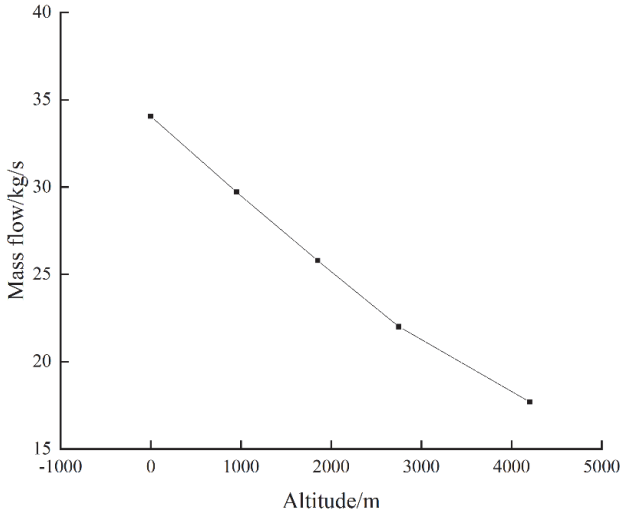

Figure 6 Smoke mass flow at smoke outlet under different altitudes in case of a 20 MW fire source power

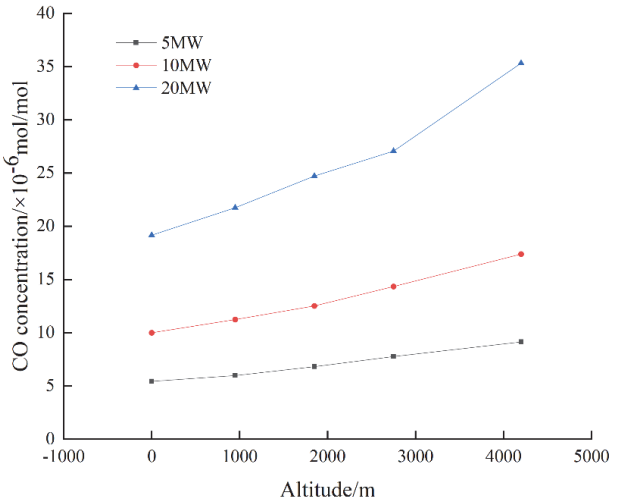

Figure 7 CO concentration of smoke outlet at different altitudes

Because the smoke outlet has an entrainment effect, the discharged smoke may contain fresh air, so it is more accurate to use the CO concentration at smoke outlet to indicate the smoke exhaust efficiency. Fig. 7 shows the changes in the CO concentration at smoke outlet at different altitudes in case of different fire source powers. According to the figure, the concentration of CO discharged from smoke outlet increases with the altitude, but in case of different fire source powers, the increment is slightly different. As the altitude increases, the curve of CO concentration becomes steeper. As the power of fire source increases, the concentration of CO discharged from the smoke outlet increases gradually, and the slope of the CO concentration curve increases as well. This is because the greater the power of the fire source, the more smoke generated within unit time, and the greater the horizontal

inertial force of the smoke. As a result, the chimney effect of the smoke outlet needs to overcome more horizontal inertial force of the smoke, so less air will be sucked in, which will result in a greater amount of discharged smoke, and the CO concentration of the smoke outlet will increase accordingly.

4 INFLUENCE OF SMOKE OUTLET SIZE ON SMOKE EXHAUST EFFECT OF HIGH-ALTITUDE TUNNELS

4.1 Analysis of Temperature at the Characteristic Height of Human Eye

Because of the low-pressure and low-oxygen environment in high altitude areas, once a fire breaks out in the tunnel, the smoke temperature will be significantly higher than that in plain areas, and this will pose great threats to the lives of people in the tunnel, thus it is necessary to set a reasonable size of smoke outlet to control the smoke temperature within a safe range. In this paper, the altitude was set to 4200 m, the characteristic height of human eye was set as 2 m, and a temperature at the characteristic height less than 60 ℃ was taken as the standard for safe evacuation.

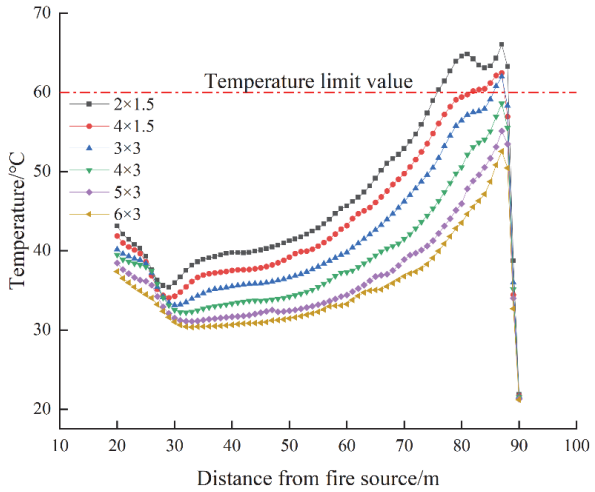

Figure 8 Smoke temperature of different smoke outlets at characteristic height

Fig. 8 shows the smoke temperature distribution at 2 m height positions under the condition of a 20 MW fire source power and different smoke outlets, as shown in the figure. With the increase of the distance from fire source, the smoke temperature at characteristic height decreases first and increases later, the main reason is that when the smoke moves to the position that is 30 m away from the center point of the fire source, the smoke outlet has an entrainment effect, so the temperature near the 30 m position declines a little bit. The temperature curves of different smoke outlets basically have the same features, when the area of smoke outlet increases, the temperature at characteristic height decreases accordingly; when the size of smoke outlet is larger than 3 × 3 m, the temperature along the escape route is lower than 60 °C, which meets the standard of safe evacuation. Considering that a too large area of smoke outlet would result in high roof temperature, the smoke exhaust effect is the best when the size of smoke outlet is 4 × 3 m. Fig. 9 gives the curves of peak temperature at the characteristic height under the condition of different smoke outlet areas. According to the figure, with the increase of the area of smoke outlet, the peak temperature at characteristic height tends to decrease. The fitting formula was attained via the least square method as $y = -0.88292x + 68.72286$, when $R^2 = 0.97738$, the fitting effect is good.

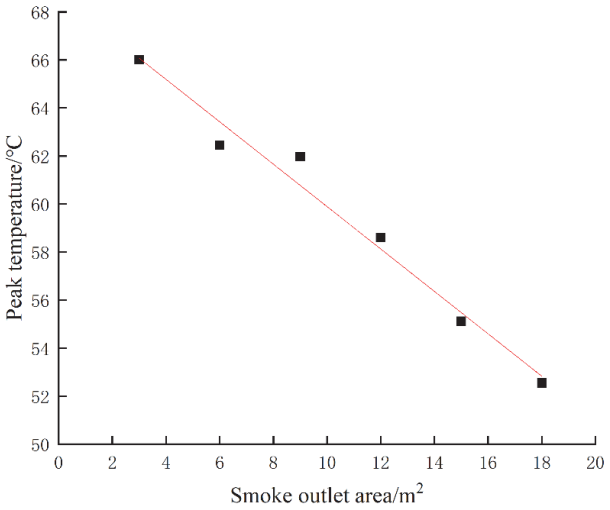

Figure 9 Distribution of peak temperature of different smoke outlets at characteristic height at 200 m altitude

4.2 CO Concentration and Visibility at Characteristic Height

During highway tunnel fire disaster, CO is one of the most harmful gases to human body, its concentration must be controlled within a reasonable range to ensure safe evacuation, so in this paper, a CO concentration of 250×10^{-6} mol/mol was taken as the standard of safe evacuation. Fig. 10 shows the distribution of CO concentration of different smoke outlets at characteristic height at 4200 m altitude. As can be clearly seen in the figure, as the distance from the center point of fire source increases, the CO concentration at characteristic height increases with it and the CO concentration values of different smoke outlets are all less than 250×10^{-6} mol/mol, which meets the requirement of safe evacuation.

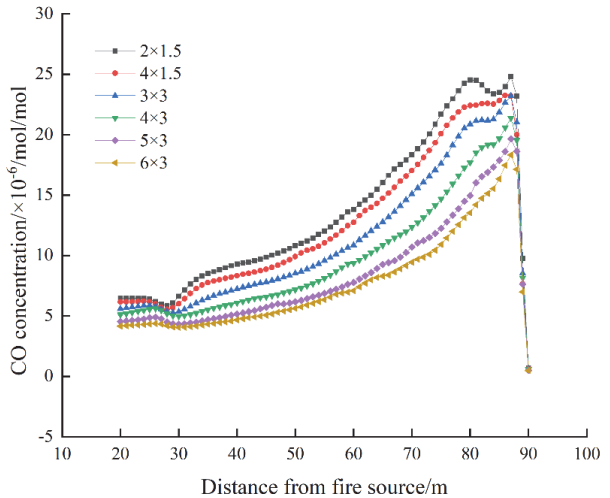

Figure 10 CO concentration of different smoke outlets at characteristic height at 4200 m altitude

Fig. 11 shows the distribution of visibility of different smoke outlets at characteristic height at 4200 m altitude.

As can be seen from the figure, the distribution laws of the visibility curves of different smoke outlets are the same, that is, as the distance from the center point of fire source increases, the visibility at characteristic height increases first and decreases later.

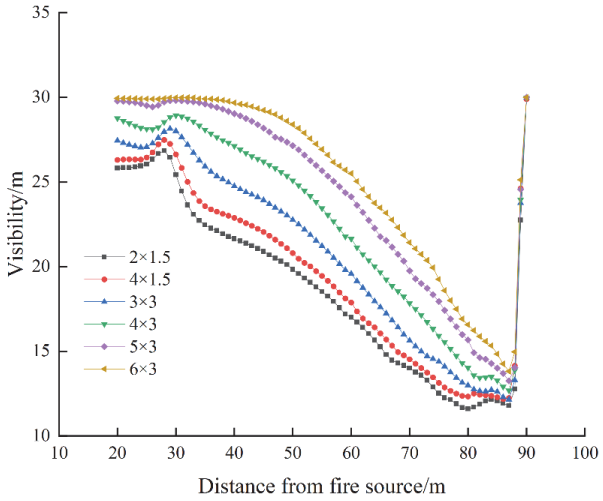

Figure 11 Visibility of different smoke outlets at characteristic height at 4200m altitude

The visibility of different smoke outlets is more than 10 m, as can be seen from the figure, the larger the area of smoke outlet, the greater the visibility at characteristic height, and the values of visibility are all greater than 10 m, which meets the standard of safe evacuation. This is because the greater the area of smoke outlet, the stronger the capacity of smoke gas entrainment, then more smoke could be discharged. As a result, at the characteristic height, the CO concentration will decrease and the visibility will be improved.

5 CONCLUSIONS

This paper used FDS to study the effects of altitude and smoke outlet size on semi-lateral smoke exhaust of highway tunnels and gave a comprehensive analysis. By setting different altitudes and smoke outlet sizes, the laws of smoke diffusion, roof temperature, and the smoke temperature, CO concentration, and visibility at characteristic height were figured out. The results show that:

(1) Under the condition of a same fire source power, as the altitude increases, the smoke spreads faster; the high-temperature zones of different altitudes are the same, and the acceleration of smoke spread brings greater challenges to the prevention and control of fire, therefore, for high altitude areas, it is suggested to use smoke detectors that are more sensitive than those used in plain areas.

(2) Under the condition of a same fire source power and different altitudes, the curves of roof temperature of different altitudes are of the same trend, the higher the altitude, the higher the roof temperature of the tunnel away from the center point of the fire; in case of the same altitude, the greater the fire source power, the higher the roof temperature.

(3) When the fire source power is 20 MW, the smoke mass flow discharged from the smoke outlet decreases with the increase of altitude; compared with the smoke mass flow at 0m altitude, the smoke mass flow at 4200 m altitude decreases by 50.1%; the CO concentration of the smoke outlet increases with the altitude; at the same altitude, the greater the fire source power, the greater the CO concentration of the smoke outlet.

(4) At 4200 m altitude, as the area of smoke outlet increases, the temperature and CO concentration at the characteristic height in the tunnel both decrease and the visibility at the characteristic height in the tunnel increases; to meet the requirement of safe evacuation, the optimal size of the smoke outlet is 4 × 3 m.

6 REFERENCES

[1] Zhang, L., Yan, Z., Li, Z., Wang, X., Han, X., & Jiang, J. (2018). Study on the effect of the jet speed of air curtain on smoke control in tunnel. *Procedia Engineering*, *211*, 1026-1033. https://doi.org/10.1016/j.proeng.2017.12.106

[2] Gong, J.., Lin, Z.., & Hua, S. (2022). Influence of ambient pressure over natural smoke ventilation in shaft tunnel fire. *International Journal of Safety and Security Engineering*, *12* (2), 185-191. https://doi.org/10.18280/ijsse.120206

[3] Liu, B., Mao, J., Xi, Y., & Hu, J. (2021). Effects of altitude on smoke movement velocity and longitudinal temperature distribution in tunnel fires. *Tunnelling and Underground Space Technology*, *112*, 103850. https://doi.org/10.1016/j.tust.2021.103850

[4] Xu, T., Tang, F., Xu, X., & He, Q. (2021). Impacts of ambient pressure on the stability of smoke layers and maximum smoke temperature under ceiling in ventilated tunnels. *Indoor and Built Environment*, 32(1), 1420326X211013080. https://doi.org/10.1177/1420326X211013080

[5] Liu, B., Mao, J., Xi, Y., & Hu, J. (2023). Effect of altitude on vertical temperature distribution and longitudinal smoke layer thickness in long tunnel fires. *Fire and Materials*, *47*(1), 16-27. https://doi.org/10.1002/fam.3065

[6] Tan, T., Yu, L., Ding, L., Gao, Z., & Ji, J. (2021). Numerical investigation on the effect of ambient pressure on mechanical smoke extraction efficiency in tunnel fires. *Fire Safety Journal*, *120*, 103136. https://doi.org/10.1016/j.firesaf.2020.103136

[7] Yan, G., Wang, M., Yu, L., Duan, R., & Xia, P. (2020). Effects of ambient pressure on smoke movement patterns in vertical shafts in tunnel fires with natural ventilation systems. *Building Simulation*, *13*, 931-941. https://doi.org/10.1007/s12273-020-0631-4

[8] Ji, J., Guo, F., Gao, Z., & Zhu, J. (2018). Effects of ambient pressure on transport characteristics of thermal-driven smoke flow in a tunnel. *International Journal of Thermal Sciences*, *125*, 210-217. https://doi.org/10.1016/j.ijthermalsci.2017.11.027

[9] Huang, R., Wu, E., Wu, L. (2020). Study on the influence of altitude on smoke propagation law in mine roadway fire.*Gold Science and Technology*, *28*(2), 293-300.

[10] Wieser, D., Jauch, P., & Willi, U. (1997). The influence of high altitude on fire detector test fires. *Fire Safety Journal*, *29*(2-3), 195-204. https://doi.org/10.1016/S0379-7112(96)00042-2

[11] Li, H., Yao, W., Li, P., Zhou, Z., & Wang, J. (2017). Influence of high altitude on combustion efficiency and radiation fraction of hydrocarbon fires. *Heat Transfer Research*, *48*(10), 865-875. https://doi.org/10.1615/HeatTransRes.2016010282

[12] Wang, J., Pan, Y., Lu, S., Lu, K., & Chen, W. (2017). CO concentration decay profile and ceiling jet entrainment in aircraft cargo compartment fires at reduced pressures. *Applied Thermal Engineering*, *110*, 772-778.

https://doi.org/10.1016/j.applthermaleng.2016.08.213
[13] Zhou, Z., Wang, J., Liu, J., Li, H., & Yuen, R. (2016). Effect of the ambient pressure on the heat release rates of n-heptane pool fires. *Journal of Thermal Analysis and Calorimetry*, *126*, 1727-1734. https://doi.org/10.1007/s10973-016-5620-6
[14] Chen, M., Liu, J., Ouyang, D., & Wang, J. (2019). Experimental investigation on the effect of ambient pressure on thermal runaway and fire behaviors of lithiumion batteries. *International Journal of Energy Research*, *43*(9), 4898-4911. https://doi.org/10.1002/er.4666
[15] He, J., Huang, X., Ning, X., Zhou, T., Wang, J., & Yuen, R. K. K. (2022). Modelling fire smoke dynamics in a stairwell of high-rise building: Effect of ambient pressure. Case Studies in Thermal Engineering, *32*, 101907. https://doi.org/10.1016/j.csite.2022.101907
[16] Chen, X., Sun, Q., Wang, H., Xie, S., Liu, Y., & He, Y. (2019, October). The effect of pressure in cruise phase on the thermal runaway behaviors and smoke components. *2019 9th International Conference on Fire Science and Fire Protection Engineering (ICFSFPE)*, 1-5. https://doi.org/10.1109/ICFSFPE48751.2019.9055814
[17] Liu, J., Zhou, Z., & Chen, M. (2019). Experimental investigation on the effect of ambient pressure on entrainment coefficient of pool fires. *Applied Thermal Engineering*, *148*, 939-943. https://doi.org/10.1016/j.applthermaleng.2018.11.110
[18] Wang, J., Fan, Y., Kong, X., & Jiang, X. (2022). Effect of reduced ambient pressure on the smoke layer of fire in shaft natural exhaust tunnel. *Safety and Environmental Engineering*, *29*(6), 78-86. https://doi.org/10.13578/j.cnki.issn.1671-1556.20211356
[19] Chaabat, F., Salizzoni, P., Creyssels, M., Mos, A., Wingrave, J., Correia, H., & Marro, M. (2020). Smoke control in tunnel with a transverse ventilation system: An experimental study. *Building and Environment*, *167*, 106480. https://doi.org/10.1016/j.buildenv.2019.106480
[20] Hao, H. & Zhang, G. (2021). Study on parameters setting of semi transverse smoke exhaust in subway tunnel. *IOP Conference Series: Earth and Environmental Science*, *825*(1), 012039. https://doi.org/10.1088/1755-1315/825/1/012039
[21] Li, Y., Mu, S., Ni, X., Niu, Z., & Tang, K. (2022). Effects of the layout of exhaust port on the performance of smoke control for ultra-wide immersed tube tunnel. *Green Connected Automated Transportation and Safety: Proceedings of the 11th International Conference on Green Intelligent Transportation Systems and Safety*, 83-95. https://doi.org/10.1007/978-981-16-5429-9_6
[22] Xu, P., Zhu, D., Xing, R., Wen, C., Jiang, S., & Li, L. (2022). Study on smoke exhaust performance in tunnel fires based on heat and smoke exhaust efficiency under the lateral centralized mode. *Case Studies in Thermal Engineering*, *34*, 102002. https://doi.org/10.1016/j.csite.2022.102002
[23] National Fire Protection Association. (2011). NFPA 502, Standard for road tunnels, bridges, and other limited access highways. NFPA.
[24] Zhang, X., Wan, X., Peng, R., Jia, B., & Lou, Q. (2020). Research on smoke prevention and control of tunnel fire under cooperation of water curtain and smoke exhaust system. *Journal of Safety Science and Technology*, *16*(7), 106-111. https://doi.org/10.11731/j.issn.1673-193x.2020.07.017
[25] McGrattan, K. B., Forney, G. P., Floyd, J., Hostikka, S., & Prasad, K. (2005). *Fire dynamics simulator (version 4) - user's guide.* US Department of Commerce, Technology Administration, National Institute of Standards and Technology.
[26] TB 10020-2017. (2017). Code for design on rescue engineering for disaster prevention and evacuation of railway tunnel. China Standards Database.

Contact information:

Xiaohua JIN
(Corresponding author)
School of Energy & Environment,
Zhongyuan University of Technology,
Zhengzhou 450007, China
E-mail: 6561@zut.edu.cn

Zhihao LIN
School of Energy & Environment,
Zhongyuan University of Technology,
Zhengzhou 450007, China

Shunheng HUA
School of Energy & Environment,
Zhongyuan University of Technology,
Zhengzhou 450007, China

Xinru TONG
School of Energy & Environment,
Zhongyuan University of Technology,
Zhengzhou 450007, China

Xiaoyan LI
School of Energy & Environment,
Zhongyuan University of Technology,
Zhengzhou 450007, China

Lingbo ZHANG
School of Energy & Environment,
Zhongyuan University of Technology,
Zhengzhou 450007, China

Jiankun GONG
School of Energy & Environment,
Zhongyuan University of Technology,
Zhengzhou 450007, China